Swelling of L α -Phases by Matching the Refractive Index of the Water−Glycerol Mixed Solvent and that of the Bilayers in the Block Copolymer System of (EO) 15 −(PDMS) 15 −(EO) 15

ARTICLE *in* THE JOURNAL OF PHYSICAL CHEMISTRY B · JUNE 2007

Impact Factor: 3.3 · DOI: 10.1021/jp0706331 · Source: PubMed

Swelling of L_α-Phases by Matching the Refractive Index of the Water−Glycerol Mixed Solvent and that of the Bilayers in the Block Copolymer System of $(EO)_{15}-(PDMS)_{15}-(EO)_{15}$

Yun Yan,*,† Heinz Hoffmann,*,† Alona Makarsky,‡ Walter Richter,§ and Yeshayahu Talmon‡

University of Bayreuth, BZKG, Bayreuth, 95448, Germany, Department of Chemical Engineering, Technion−Israel Institute of Technology, Haifa 32000, Israel, and Klinikum der FSU Jena, Elektronenmikroskopisches Zentrum, Ziegelmühlenweg 1, 07740 Jena, Germany

Received: January 25, 2007; In Final Form: March 14, 2007

The swelling of L_α-phases from the block copolymer polyethylenoxide−b-polydimethylsiloxane−polyethylenoxide $(EO)_{15}-(PDMS)_{15}-(EO)_{15}$ in water/glycerol mixtures is reported. At low and medium polymer concentrations (<60%), the block copolymer forms a turbid vesicular dispersion in water. With time, the small unilamellar vesicles (SUV) and the large multilamellar vesicles (MLV) separate into a two phase L_1/L_α-system. The turbid dispersions of the L_α-phase below 60% of the compound become more and more transparent with increasing glycerol and at 60% of glycerol become completely clear. Replacement of water by the solvent glycerol thus lowers the turbidity of the dispersion and swells the interlamellar distance between the bilayers. A 20% aqueous L_1/L_α-dispersion can thus be transformed into a single birefringent transparent L_α-phase. The swelling of the L_α-phase in water and the decrease of the turbidity of the dispersion by the addition of glycerol is explained by the matching of the refractive index of the solvent to the refractive index of the bilayers of the block copolymer. The matching of a refractive index lowers the Hamaker constant in the DLVO theory between the bilayers and therefore decreases the attraction between the bilayers what allows them to swell to a larger separation. The microstructures in the phases were determined by cryo- and FFR-TEM. The interlamellar distance between the bilayers was determined by SAXS measurements. The viscous properties of the L_α-phases were determined by oscillatory rheological measurements. In comparison to other L_α-phases from normal surfactants, the L_α-phases from the block copolymer $(EO)_{15}-(PDMS)_{15}-(EO)_{15}$ have low shear moduli. This is probably due to the high flexibility of the poly dimethylsiloxane block in the bilayers what can be recognized on the non-spherical shapes of the SUV's.

Introduction

Siloxane surfactants with polydimethyl siloxane (PDMS) structure find many commercial applications[1−7] (as additives in cosmetics, textile manufacture, wetting and coating agents and as agricultural adjuvants) which emanate from their unique surface activity in both aqueous and nonaqueous media.[8] The dimethyl−siloxane backbones are flexible and usually coil, which leads to a dense packing of methyl groups at the air/water interface. The dense methyl groups together with the low cohesion forces between siloxanes enable these surfactants to have low surface tensions above the CMC (critical micellization concentration).[9]

Recently, the aggregation behavior of some siloxane surfactants in water has been reported.[10−16] At high concentrations (e.g., >50%), the siloxane surfactants usually form lyotropic liquid crystalline structures, much like typical hydrocarbon surfactants,[10,14,16] whereas at low concentrations[13,16] (e.g., <10%) they can form an unusual diversity of spherical and wormlike micelles, as well as tube-like, unilamellar, and multilamellar vesicles.

* Corresponding authors. H.H.: e-mail, heinz.hoffmann@nmbgmbh.de; tel, +49-921-50736-135; fax, +49-921-50736-139. Y.Y.: e-mail, yun.yan@wur.nl; tel, +31-317-485648; fax, +31-317-483777.
† University of Bayreuth.
‡ Technion−Israel Institute of Technology.
§ Elektronenmikroskopisches Zentrum.

However, the application of siloxane surfactants is inevitably in combination with glycerol, because surfactant aggregates in mixed solvents, rather than in pure water, have extensive application in everyday life.[17] For instance, the formulations of pharmaceutical recipes, personal care products, detergents, and foods often contain glycerol to improve its sensory perception.[18] Therefore, it is important to know the aggregation and phase behavior of siloxane surfactants in glycerol−water mixed solvents.

There are several reports about the effect of glycerol−water mixed solvent on the micellization and the phase behavior of amphiphiles.[19−26] It has been found that the CMC of surfactants is higher in the mixed solvents than in pure water, and even exponentially increases with increasing glycerol concentration.[27−29] The substitution of water by glycerol in water/C_mEO_n/hydrocarbon system can induce the transition of oil-in-water (O/W) to water-in-oil (W/O) microemulsions.[30] In the pluronics/water system, the addition of ethyleneglycol increases the lattice spacing of the liquid crystalline structures.[31] Lin and Alexandridis also reported that increased glycerol content in the mixed solvent leads to the formation of ellipsoidal micelles in a PDMS-graft-polyether copolymer system.[23] However, the published information on the effect of glycerol on the solution behavior of surfactants is rather limited; especially, no systematic research about the effect of glycerol on the aggregation and phase behavior of siloxane surfactants has been reported. Such lack

10.1021/jp0706331 CCC: $37.00
Published on Web 05/10/2007

of fundamental knowledge is in contrast to the current trend of increasing commercial use of these surfactants. Therefore, in this research we attempt to shed some light on the aggregation and phase behavior of siloxane surfactant in water−glycerol mixed solvents.

The surfactant we used is the ABA type nonionic triblock-copolymer siloxane surfactant, polyethyleneoxide-b-polydimethylsiloxane-b-polyethyleneoxide, i.e., $[(EO)_{15}-(PDMS)_{15}-(EO)_{15}]$, commercially named IM-22. We first studied the phase behavior of IM-22 in water/glycerol mixtures, and followed the change of aggregate nanostructure with increasing glycerol fraction in the solvent. By using direct-imaging cryo-TEM and freeze-fracture-replication (FFR)-TEM, we found that the vesicles in dilute IM-22 solutions are broken with increasing the volume of glycerol. SAXS results indicate the interlamellar distance between the bilayer swells with increasing the glycerol concentration. The viscous properties of the phases, determined by oscillatory rheological measurements, agree well with the TEM and SAXS results. The effect of glycerol on the phase and aggregation behavior of the IM-22 water system was explained by the vanishing of the attraction between the bilayers with increasing glycerol.

Materials and Methods

Materials The siloxane surfactant $[(EO)_{15}-(PDMS)_{15}-(EO)_{15}]$, i.e., IM-22, was a gift from Wacker Company, and was used without further purification. Anhydrous glycerol (99.5%) and distilled water were used throughout the experiments.

Methods. *Phase Diagram.* The samples were prepared by vortex mixing IM-22−water−glycerol systems in 10 mL test tubes. Air bubbles were removed by centrifugation. The phase diagram was established by observing the solutions in test tubes under temperature-controlled conditions after several weeks. The phases were characterized by visual inspection with and without polarizers. The concentration of IM-22 is expressed in weight percent (wt%), while the content of glycerol in glycerol−water mixed solvent refers to volume percent to keep the same volumes for all the samples. The mixing ratios of glycerol to water are also in terms of volume ratio.

Refractive Index. The refractive index of the glycerol−water mixtures was obtained from Borst et al.[32] A master curve was established based on these reference values. From that, refractive index for the 60% glycerol (V%) system, corresponding to the mass ratio of 0.65, is 1.420. The master curve for PEO-PDMS system was established based on the refractive indexes of the pure PEO and pure PDMS, which are 1.569[33] and 1.400[34] at 598 nm, respectively. Therefore, the refractive index values of PEO-PDMS block copolymer against different EO mass ratios were plotted. The IM-22 was calculated to have an EO-PDMS ratio of 0.53, which corresponds to a refractive index of 1.426 ± 0.005 on the master curve.

Cryo-Transmission Electron Microscopy (cryo-TEM). Vitrified specimens for cryo-TEM were prepared in a controlled environment vitrification chamber and quenched into liquid ethane at its freezing point.[35] Specimens, kept below −178 °C, were examined in a Philips CM120 microscope, operated at 120kV, using an Oxford CT-3500 cryo-holder system. Images were recorded digitally in the minimal electron dose mode by a Gatan 791 Multiscan CCD camera with the Digital Micrograph software package.

Freeze-Fracture-Replication Transmission Electron Microscopy (FFR-TEM) For the FFR-TEM experiment, a small amount of sample was placed on a 0.1 mm thick copper disk covered with a second copper disk. The sample was frozen by plunging this sandwich into liquid propane, which had been cooled by liquid nitrogen. Fracturing and replication were carried out in a freeze-fracture apparatus (Balzers BAF 400, Germany) at a temperature of −140 °C. Pt/C was sputter-coated at an angle of 45° and backed with a carbon layer. The replica was examined in a CEM 902 electron microscope (Zeiss, Germany).

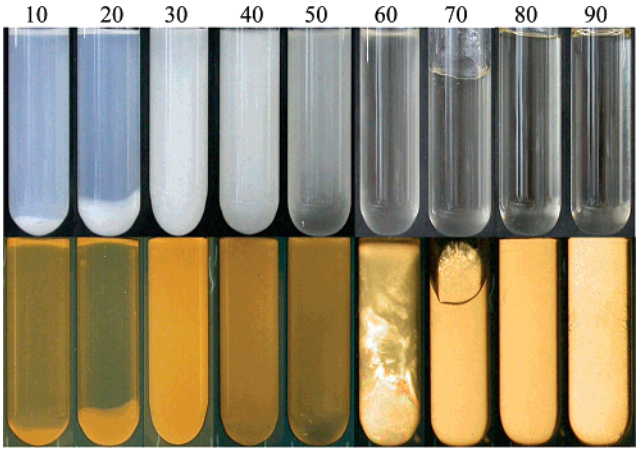

Figure 1. Phase behavior of IM-22 in water (25 °C) observed without polarizers (upper samples) and with crossed polarizers (lower samples). The numbers above the photos are the concentration of IM-22 aqueous solution (wt%).

Rheological Measurements. The rheological measurements were performed by a Haake RS600 with a cone and plate sensor, and a Haake RS300 with a double-gap cylinder sensor. The sensor systems can be chosen according to the fluidity of the sample: RS600 for highly viscous liquids and RS300 for low viscosity liquids (<100 mPa s). Temperature in the measuring system was controlled to ±0.1 °C by a thermo-controller (Haake TC 81) for the RS600, and by an ethylene glycol circulator with an accuracy of ±0.5 °C for the RS300. The viscous properties were determined by steady-state shear rate ramping, and the viscoelastic properties by oscillatory measurements from 0.01 to 10 Hz, for which the deformation was controlled to be in the linear region.

Small-Angle X-Ray Scattering (SAXS). SAXS measurements were performed on a Kratky compact small-angle system equipped with a position-sensitive detector (OED 50M, Mbraun, Graz, Austria) consisting of 1024 channels of 53.0 μm width each. The camera volume was kept under vacuum during the measurements in order to minimize the background scattering from air. The temperature was kept at 25 °C by a Peltier element. The sample holder was a 1 mm quartz capillary which was filled with the samples by a syringe.

Results

1. Phase Diagrams. *1.1. Phase Diagrams of IM-22 in Water.* Photos of the samples with increasing concentration of IM-22 are given in Figure 1. All samples from 10−50% of IM-22 are turbid. The samples separate macroscopically into two phases on standing for long times (weeks), with a lower birefringent phase and an upper isotropic phase. The phases with 60% to 90% are single transparent birefringent phases. The pure IM-22 sample is a clear isotropic viscous phase.

1.2. Influence of Glycerol on the Two-Phase System with 20% IM-22. In Figure 2 photos of samples with 20% of the block copolymers are shown in glycerol−water mixtures. In water the block copolymer phase (L_α-phase) is at the bottom of the test tube, while with 10% glycerol the compound is at the top

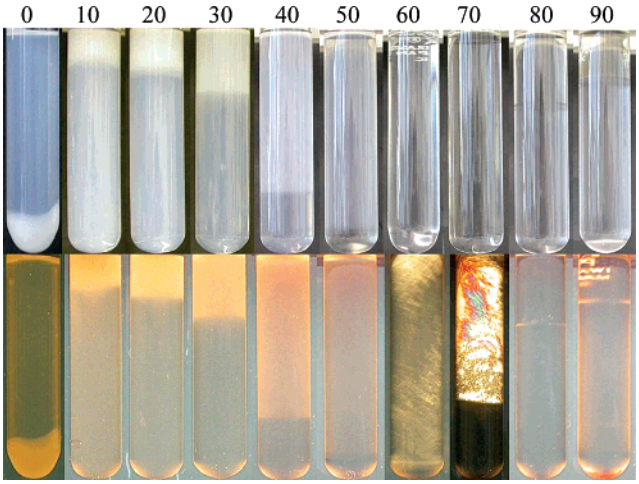

Figure 2. Photos for 20% IM-22 in water−glycerol mixed solvents. The numbers above the photos are the volume percent (V%) of glycerol in water−glycerol mixture. Upper samples: without polarizers. Lower samples: with crossed-polarizers.

of the test tube. The density of the L_α-phase is obviously larger than the density of pure water, but smaller than in a water−glycerol mixture with 10% of glycerol. With increasing glycerol content, the volume of the L_α-phase swells until at a glycerol volume of 60%, the system becomes a single L_α-phase that is completely clear. In the 70% system, the system turns again into a two-phase L_1/L_α situation, while the last two mixtures are isotropic solutions. The described behavior of the system brings up the question why does the L_α-phase in the L_1/L_α two-phase situation swell upon glycerol addition. Obviously, at equilibrium the repulsive and attractive forces are compensating each other at a well-defined spacing between the bilayers. This interlamellar distance increases with glycerol content. For uncharged systems the repulsion between the bilayers results from undulation forces and the attraction between the bilayers comes from general van der Waals forces. It could be argued that the undulation forces become larger with increasing glycerol content because the bilayers very likely become more flexible with increasing the glycerol content. The addition of glycerol to nonionic surfactant systems lowers the solvation of the headgroups, what should lower the stiffness of the bilayer.[30,31]

The imbalance of the forces in the L_α-phase with the glycerol content could also come from a lowering of the attraction between the bilayers. This conclusion is actually supported from the appearance of the samples with increasing glycerol content. The samples become less turbid and at 60% system become completely clear. This decrease of turbidity must come from a matching of the refractive index of the mixed solvent with the refraction index of the block copolymer. The van der Waals forces reflect this difference of the reflective index between solvent and structure, and, at the matching point the van der Waals forces between the bilayers vanish.

1.3. Influence of Glycerol on the System with 5% IM-22. Photos of 5% IM-22 with increasing glycerol are given in Figure 3. In water, the solution is turbid bluish single phase without birefringence. This turbid solution is stable for several weeks at 25 °C. The solution contains SUVs and MLVs as will be shown in section 3. At longer times the turbid solution separates into a turbid birefringent lower phase and a more-or-less transparent upper phase. The turbid solution is thus a thermodynamically unstable dispersion of a L_α-phase. With increasing glycerol from 10% to 60%, the turbidity decreases and, at 60% glycerol content, the sample becomes totally transparent. As concluded in the 20% IM-22 system, this decrease of turbidity is an indication of the matching of refractive index of the bilayers of IM-22 with the refractive index of the mixed solvent. However, it could also be a sign that the vesicles in the system disappear. In glycerol range of 70−90%, isotropic phase separation with the upper phase less than 15% of the bulk volume is found. Both the upper and lower phases are transparent and have no birefringence at 25 °C. However, birefringence is found for the upper phase at 5 °C, which indicates the L_α-phase (Figure 3 lower).

2. Direct Imaging cryo-TEM and FFR-TEM Results. Changes in the appearance of the samples with the addition of glycerol in dilute solutions should be reflected in direct-imaging cryo-TEM micrographs. Micrographs were therefore taken of samples with 1% and 5% IM-22 in water−glycerol mixtures. In Figure 4 we show cryo-TEM results of IM-22 in water, 20% glycerol, and 40% glycerol systems. In addition to large multilamellar vesicles (MLV) and small unilamellar vesicles (SUV) (Figure 4a), we observe also some spherical and

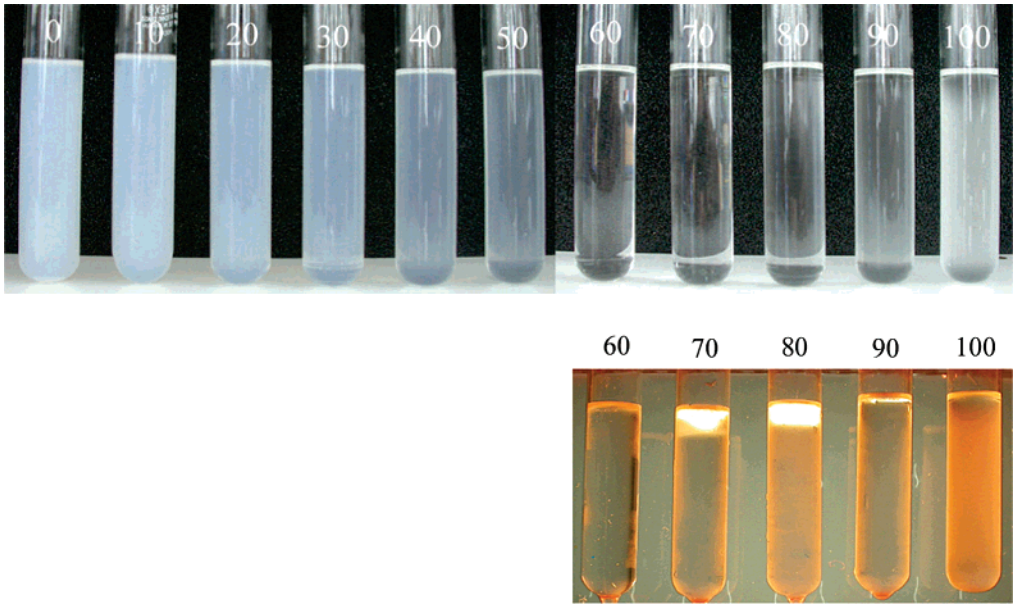

Figure 3. Photos for 5% IM-22 in water−glycerol mixed solvents. The numbers above the photos are the volume percent of glycerol. Upper samples: samples in daylight at 25 °C without polarizers. Lower samples: samples in 60−100% glycerol at 5 °C in between two polarizers.

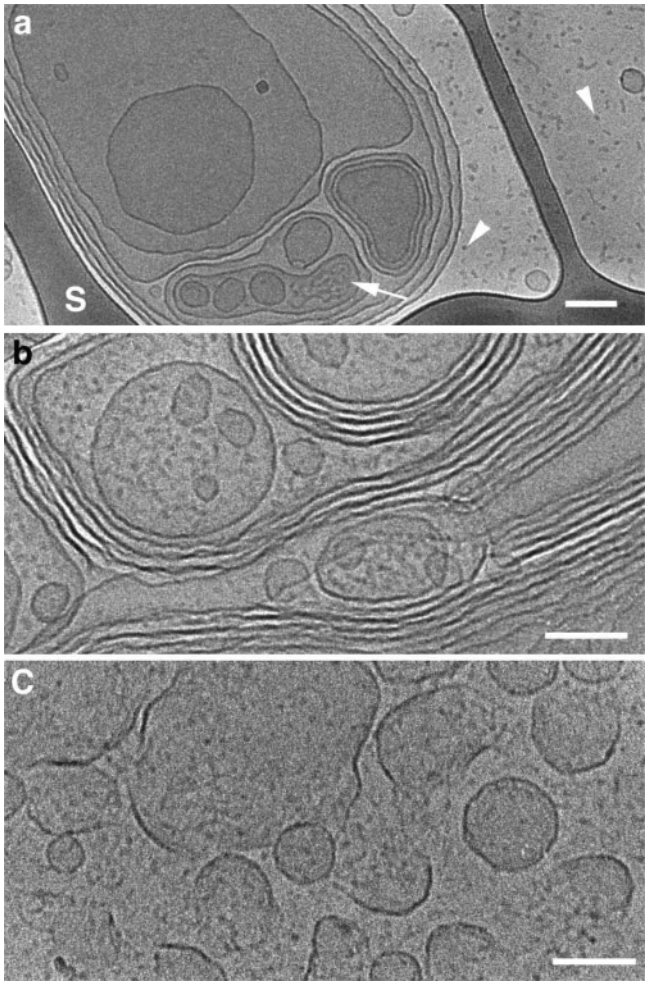

Figure 4. Direct-imaging cryo-TEM images: (a) 1% IM-22 in H_2O; arrowheads point to spherical micelles, arrow to threadlike micelles; 'S' s the support film. (b) 5% IM-22 in 20% glycerol. (c) 5% IM-22 in 40% glycerol. Bars = 100 nm.

threadlike micelles. These structures are preserved in 20% glycerol system (Figure 4b). However, they start to break down at 40% glycerol, as shown in Figure 4c. At that glycerol concentration contrast is somewhat lower than in pure water. This had been also found in cryo-TEM of quaternary ammonium surfactants in mixtures of ethylene glycol and water, as well as in glycerol−water mixtures.[36]

Unfortunately, the contrast between the microstructures and the solvent becomes very poor at high glycerol content, and the aggregates can no longer be visualized. At 60% glycerol, the contrast vanishes (Figure 5a). This means that the electron scattering ability of the solvent equals that of the aggregates, because of similar electron density. To overcome this, we use the electron beam to enhance contrast.[37] One can carefully expose the specimen to electron dose of about 20 electrons per $Å^2$, somewhat higher than that normally applied under low electron dose imaging conditions, typically less than 10 electrons per $Å^2$, as used in Figure 5a. Electron-beam radiation damage, which is faster at the organic matter−aqueous solution interface, then preferentially etches and reveals the aggregates, as seen in Figure 5b. Going back to Figure 5a and comparing it to Figure 5b, one can make out the original, undamaged structures, faintly discernible on the background of the vitrified solution. The etching process, while useful to show the aggregates, cannot give high-resolution information of those, therefore we also applied freeze-fracture-replication to these samples.

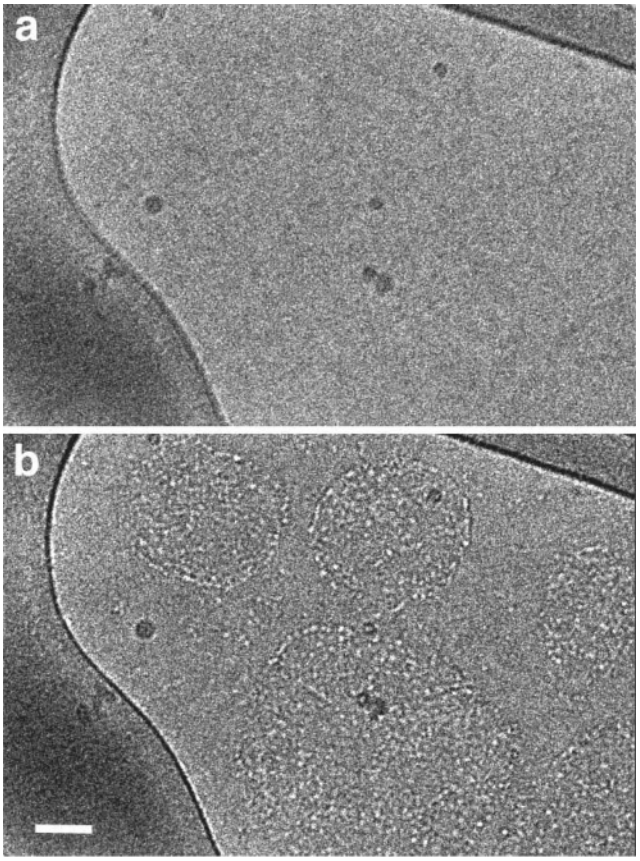

Figure 5. Direct-imaging cryo-TEM of 5% IM-22 in 60% aqueous glycerol solution. (a) Low-dose image (electron exposure $<10\ e^-/Å^2$); (b) higher electron dose image (approximately $20\ e^-/Å^2$) of same area, showing etched vesicles in the vitrified solvent. Bar = 50 nm.

Curiously the loss of contrast in the electron microscope occurs at the same glycerol concentration that leads to loss of contrast for visible light. The reason for the latter, however, is quite different. It is the result of the indices of refraction of the surfactant and solvent becoming equal, as discussed below.

Figure 6 shows the freeze-fracture images of 5% IM-22 in pure water, and 20%, 40% and 60% glycerol−H_2O mixed solvents. In pure water solution, as observed by direct-imaging cryo-TEM, both small unilamellar vesicles (SUVs) and large multilamellar vesicles (MLVs) as well as threadlike micelles are seen. The SUVs are less than 50 nm, but the MLVs are about 500 nm or even bigger. As 20% water is substituted by glycerol, the shape and size of the unilamellar vesicles does not seem to change. Note that glycerol acts as a "cryo-protectant"; thus, the contrast between structure and the background become clearer. (Indeed, 20% glycerol is sometimes added to biological samples before freeze-fracture replication). However, as the glycerol content is increased to 40%, the size of the SUVs obviously increases, as compared with those in 20% glycerol. Meanwhile, the MLVs tend to break, and some bilayer fragments are clearly seen. The most significant feature is observed in the 60% system. As revealed in Figure 6d, as the glycerol content is increased to 60%, both the SUVs less than 50 nm and the MLVs about 500 nm are no longer seen. Subsequently, large amount of broken vesicles and bilayer fragments show up. It is also clearly seen that the distance between these broken vesicles become smaller; i.e., the number density of the vesicle increases. In comparison with the 40% glycerol system, there are more large membrane fragments longer than 200 nm, which are the residues of the broken MLVs in the 60% glycerol system. Actually, the system at 60%

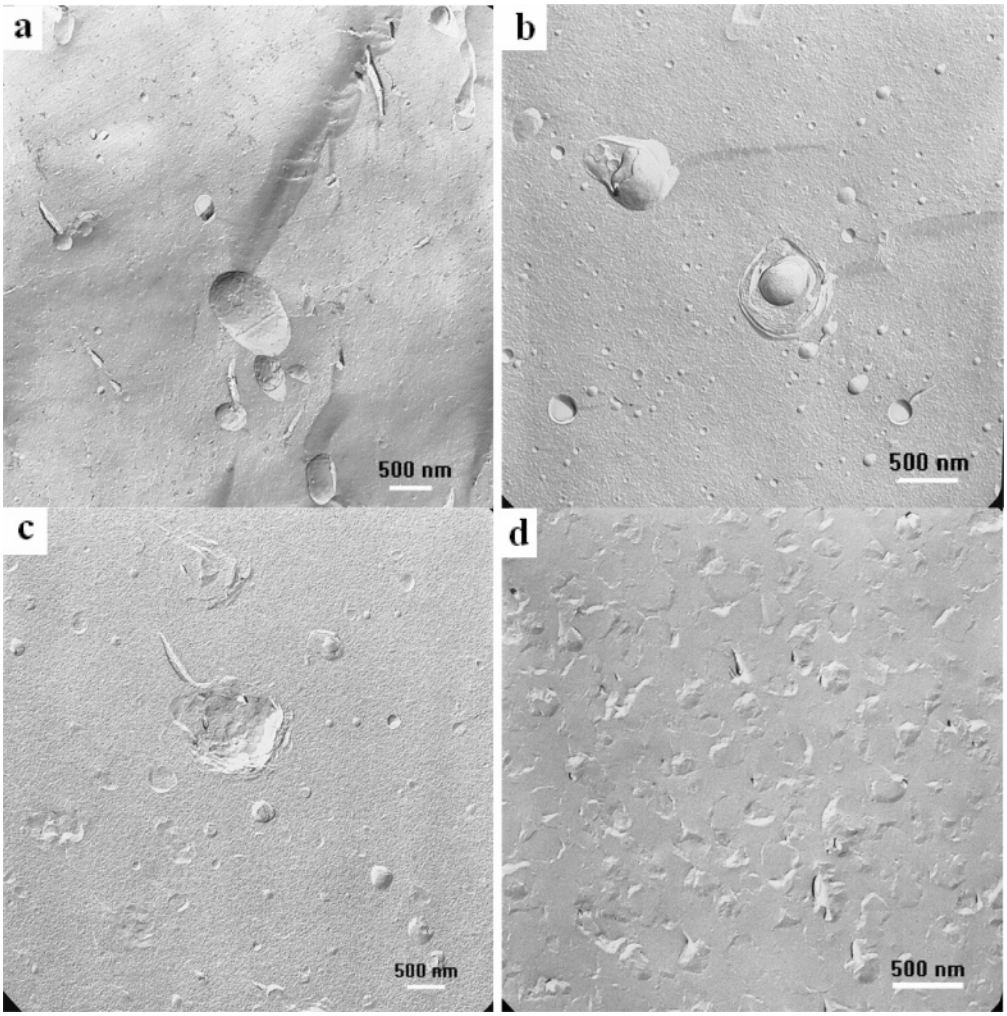

Figure 6. FFR-TEM images of IM-22 in (a) water, (b) 20% glycerol, (c) 40% glycerol, and (d) 60% glycerol.

glycerol becomes very crowded with swollen vesicles and bilayer fragments. This is a direct evidence that the small structures at 60% glycerol swell to bigger size, so they occupy the full volume of the system.

It should be noted that it is assumed that the change of the microstructures as observed by TEM and the change of the macroscopic properties (visual appearance and flow behavior) is a result only of the change of the interaction between the bilayers and not a change of the microstructure in the system. As has been revealed by the TEM results, the size of the vesicles swells as increasing glycerol, which normally should bring up a decrease in the transparency of samples; however, we observed an increase of transparency. This is also a proof that the change of the macroscopic properties is caused by the solvent property; i.e., the matching of refractive index between the solvent and that of the IM-22 molecules.

3. SAXS Ddata. *3.1. Concentration Dependence in the Glycerol Swollen L_α-Phase.* In Figure 7 we show the scattering curves at increasing concentrations of IM-22 in 60% glycerol−water mixtures against the scattering vector. The 60% mixture is the solvent in which the bilayers are present in the most swollen state. The scattering intensities show only one strong maximum and no other peaks. The single peak is an indication that the L_α-phase is not highly ordered, what is due to the strong undulations of the bilayers. The interlamellar spacing d can simply be determined from the equation

$$d = 2\pi/q_{max} \qquad (1)$$

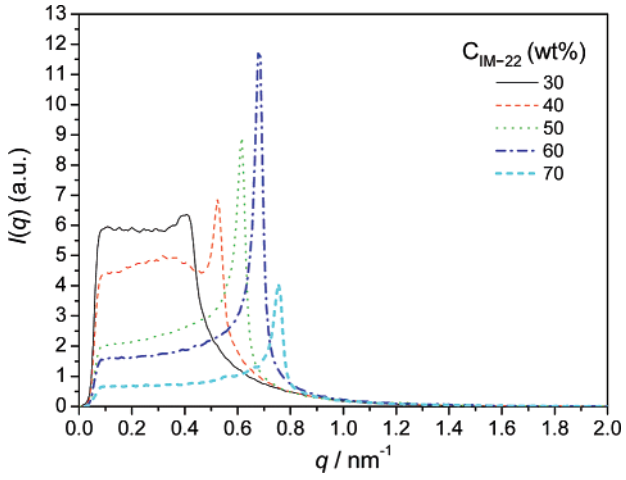

Figure 7. IM-22 in the mixed solvent of water:glycerol = 4:6 system.

where q_{max} is the first scattering peak in the SAXS measurements.

The interlamellar spacing d is related to the volume fraction of the compound, ϕ, by

$$\phi = \delta/d \quad \text{and} \quad d = \delta + D_w \qquad (2)$$

where δ is the thickness of the bilayer and D_w the thickness of the water layer when it is assumed that the density, ρ, of the

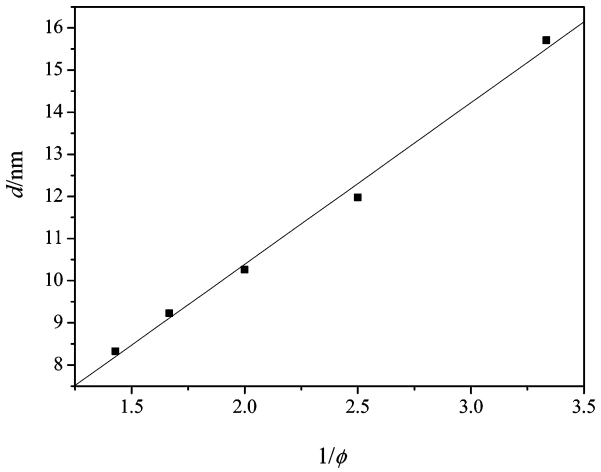

Figure 8. Interlayer spacing, d, against the mass fraction, ϕ, of IM-22 in the 4:6 water−glycerol mixes solvent.

bilayer and the solvent are about the same. The thickness of the bilayer can then be determined from the plot $d = \delta/\phi$; see Figure 8.

The plot gives a bilayer thickness of $\delta = 3.4$ nm. This rather low value for the IM-22 compound, which has a contour length of about 10.6 nm, shows that the PDMS block must be present in a rather collapsed state. It also can be concluded from eq 2 that the higher the concentration, the smaller the layer spacing. For 20% IM-22 in 4:6 (water:glycerol) system, the interlamellar spacing is about 34 nm, while it shrinks to about 8.4 nm at 70% IM-22 concentration. This is reflected by the sharper peak patterns with increasing glycerol concentration (Figure 7).

4. Rheology. *4.1. Effect of Glycerol on the Rheological Behavior of System at 20% IM 22.* The change in the macroscopic appearance and the swelling of the bilayers with increasing glycerol concentration have to be reflected in the rheological properties of these phases. The rheograms in Figure 9 show that, the complex viscosities $|\eta|^*$ for all the 20% IM-22 solutions with different contents of glycerol decrease with increasing shear frequency; i.e., the systems are shear-thinning. It should be noted that the mixed solvents are all Newtonian liquids with a viscosity that is very much lower than the complex viscosity of the samples. The rheological properties are thus due to the structures in the samples. In general, the complex viscosities decrease for a given frequency, such as at 0.01 Hz in Figure 9, with increasing glycerol content. This is a consequence of the fact that the structures become softer with increasing glycerol content. This is also reflected in the change of the storage modulus with increasing glycerol. We see in Figure 9 that at 0.01 Hz, the storage modulus G' decreases also as the glycerol content increases from 50% to 70%. It is noticeable that for all the systems with different glycerol content (50, 60, and 70%), both the storage modulus G' and the loss modulus G'' vary with shear frequency, and crossovers are found, which indicates that the L_α-phase of 20% IM-22 in water/glycerol mixtures does not behave as many studied L_α-phases which have frequency independent moduli with the storage modulus G' by a factor of 10 higher than the loss modulus G''. The rheological properties of the L_α -phase are thus very much like the properties of some viscous L_1-phases. In the 60% glycerol system, at frequencies below 0.1 Hz the L_α-phase still has frequency independent moduli with the storage modulus higher than the viscous one. This means that the system is more like typical L_α-phase. For long times or low frequencies the elastic properties dominate, with a frequency independent storage modulus of about 0.3Pa. With increasing glycerol from 50% to 60% in the system, the storage modulus decreases, which is an indication of swelling of the L_α-phase. At further increase of the glycerol content to 70%, the viscous modulus dominates the systems in the 0.01−10 Hz range, and the system behaves more like the pure compound itself. This behavior could also be due to the dehydration of the L_α-phase by the glycerol.

4.2. Flow Birefringence Phenomenon in the 60% Glycerol Solution. The swelling of the bilayers with increasing glycerol is also reflected in the dilute IM-22 vesicle solution. Although 5% IM-22 solutions with glycerol lower than 60% are all homogeneous, only in the 60% glycerol system, in which the L_α-phase is in a most swollen state, we find flow birefringence, as shown in Figure 10. The photos were shot continuously after shear (within 0.5 s). The life time for the birefringence is so short that it disappears shortly after the flow is stopped. The flow birefringent phenomenon is an indication that the swollen bilayers align under shear. As shown in FFR-TEM results, large amount of unilamellar broken vesicles about 200 nm, together with some bilayer fragments, are observed in the 60% glycerol system. The large vesicles are deformed under shear, and are aligned along the shear direction to give flow birefringence. In contrast, only a few large MLVs are observed in the 5% IM-22 solutions at glycerol concentrations lower than 40%, therefore flow birefringence is not observed due to too few bilayers.

*4.3. Rheological Properties of the Vesicle Phase.*The macroscopic flow-birefringence in a vesicle phase at specific glycerol content must be reflected in the rheological properties. The rheological properties were therefore measured from 5% samples at different glycerol concentrations. In Figure 11a the relative viscosities of 5% IM-22 in different water−glycerol mixed solvent are shown. The relative viscosity is obtained by dividing the viscosity of 5% IM-22 solution by that of the corresponding solvent. Three main characteristics can be found from this figure: (i) in 0%, 20%, and 40% glycerol, the solutions are still Newtonian fluids as is shown by the shear rate independent viscosity; (ii) the 60% glycerol system gives shear-thinning behavior, which is due to the alignment of bilayers under shear flow; (iii) the relative viscosity increases with glycerol concentration until 40% glycerol, which indicates the vesicles are still conserved till the 6:4 water:glycerol ratio, but the vesicle size has been increased.

In Figure 11b we see the rheogram of 5% IM-22 in 60% glycerol. At frequencies below 0.1 Hz the solution has a frequency independent viscosity. In the frequency range of 0.01−1 Hz, the storage and the loss moduli increase with the slopes of a Maxwell fluid, that is, with slopes of two and one. The two moduli cross at the frequency of 1 Hz. This means that the system has a structural relaxation time of $1/\omega = 1/2\pi\nu = 0.05$ s, indicating that the flow birefringence in this system disappears rapidly.

5. Discussion

The effect of glycerol on the phase and aggregation behavior of surfactant and Pluronics has been explained as the result of dehydration of amphiphiles.[30,31] It is well-known that the glycerol has strong ability to form hydrogen bonds with water. Therefore, these molecules compete with the water molecules to bind to surfactant in aqueous solution. In that way the surfactant molecules, especially nonionic surfactant, such as Pluronics and C_mEO_n, are dehydrated, and their hydrophilicity decreases. This is reflected by the phase separation of surfactants at high glycerol content. However, the swelling of the L_α-phase in our experiment leads to another explanation of the influence of glycerol on the phase behavior. It suggests that there must

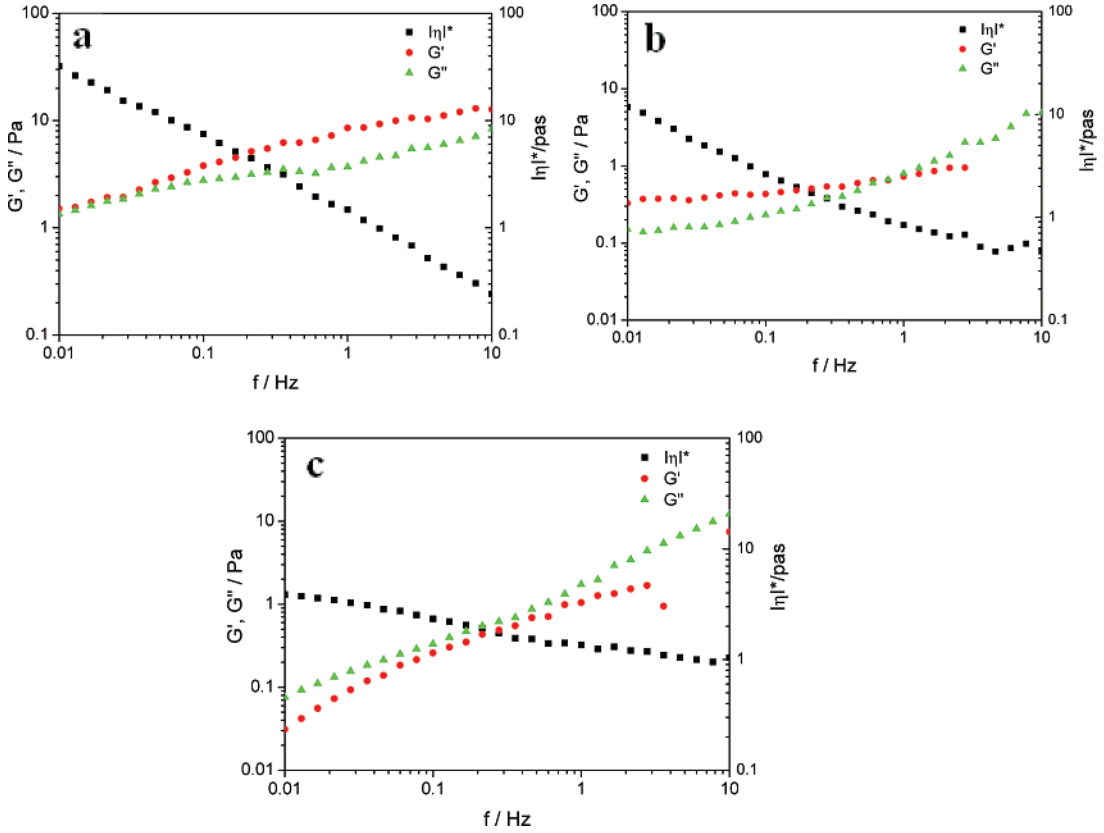

Figure 9. Dynamic rheological measurements for the 20% IM-22 in different glycerol solutions: (a) upper phase (L_α phase) of 50% glycerol; (b) 60% glycerol; (c) upper phase (L_α-phase) of 70% glycerol at 25 °C.

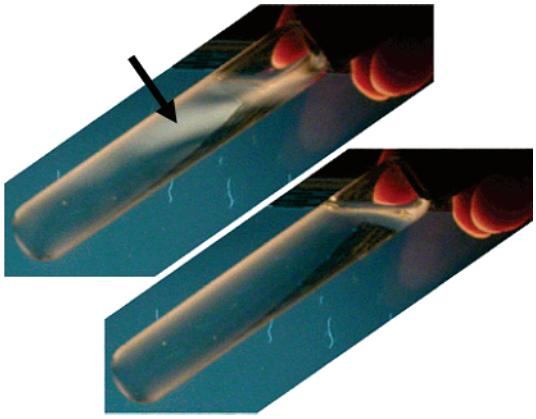

Figure 10. Flow birefringence of 5% IM-22 in 4:6 water−glycerol mixed solvent. Upper sample: immediately after up-side-down shear; the arrow clearly designates the flow birefringence. Lower sample: 0.5s later after shear; no birefringence is seen any more.

be an increase of repulsive or a decrease of attractive forces between the bilayers with increasing glycerol. Generally, in the L_α-phase the bilayers have a well-defined spacing which is the result of an equilibrium between the attractive van der Waals forces and repulsive undulation forces. The pressure of attraction per unit area for the situation, when two bilayers of thickness δ approach to a distance d ($d \gg \delta$) is given by[38]

$$P_A = -\frac{A}{6\pi}\left[\frac{1}{d^3} - \frac{2}{(d+\delta)^3} + \frac{1}{(d+2\delta)^3}\right] \qquad (3)$$

where A is the Hamaker constant, which depends on the material of the bilayer and the medium property.

For many materials, the Hamaker constant is given by the following approximate expression:[39]

$$A = \frac{3}{4}kT\left[\frac{\varepsilon_d - \varepsilon_m}{\varepsilon_d + \varepsilon_m}\right]^2 + \frac{3}{16\sqrt{2}}\hbar\omega\frac{(n_d^2 - n_m^2)^2}{(n_d^2 + n_m^2)^{3/2}} \qquad (4)$$

Here, k is Bolzman constant, T the absolute temperature, n_d and n_m are the refractive indices of the particles and the medium, respectively, for visible light, ω is the frequency of the dominating UV absorption (about $1.7-2.4 \times 10^{16}$ rad/s), and $h = 2\pi\hbar$ is Planck's constant. The quantities ε_d and ε_m are the dielectric constants of particles and the medium at zero frequency (static field). The second term in eq 4 is very much larger than the first one which is smaller than kT. The Hamaker constant A is mainly determined by the second term, i.e.:

$$A \approx \frac{3}{16\sqrt{2}}\hbar\omega\frac{(n_d^2 - n_m^2)^2}{(n_d^2 + n_m^2)^{3/2}} \qquad (5)$$

The undulation repulsion obeys the Helfrich equation (eq 6), which specifies the steric hindrance between adjacent membranes. In a multilayer system this gives rise to a repulsive pressure given by[40]

$$P_R = \frac{3\pi^2}{64}\frac{(kT)^2}{\kappa}\frac{1}{(d-\delta)^3} \qquad (6)$$

where k is the Bolzman constant, T the absolute temperature, κ the bending modulus of bilayer, δ the membrane thickness, and d is the interlayer spacing.

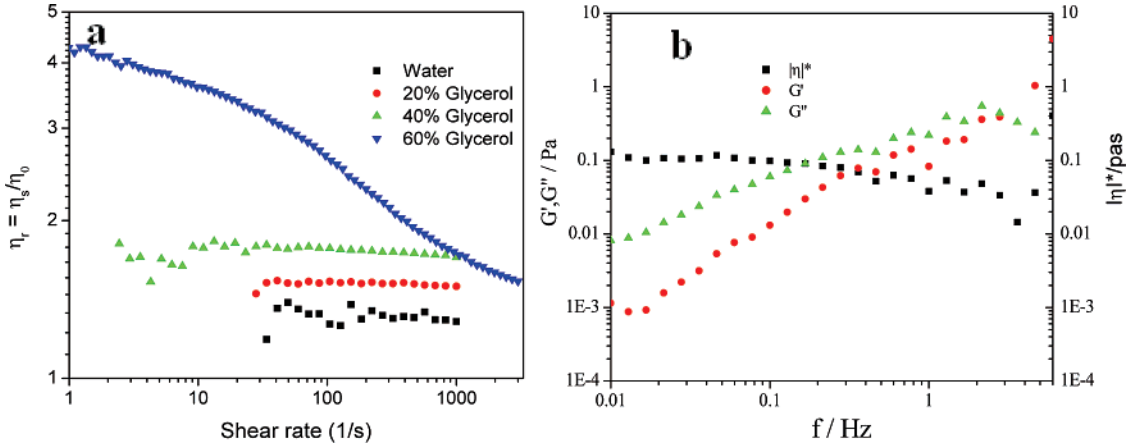

Figure 11. (a) Relative viscosity for 5% IM-22 in different solvent; (b) rheogram of the 5% IM-22 in 60% glycerol solution.

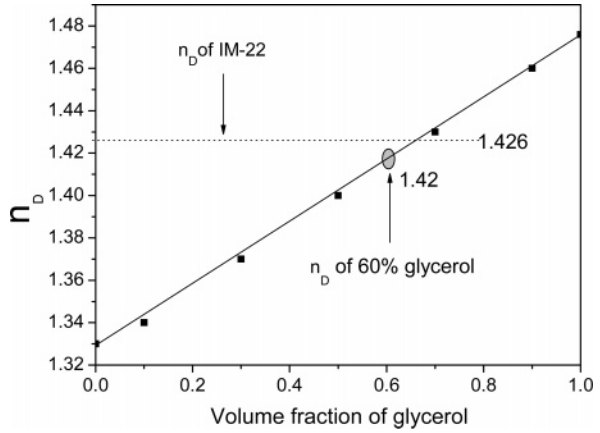

Figure 12. The refractive index, n_D, of water−glycerol mixtures and of IM-22.

With increasing the glycerol content in the mixed solvent, the refractive index of the solvent increases, and the difference between that of the IM-22 and the solvent decreases. At 60% glycerol system, the refractive index of the solvent is 1.420, which is quite close to that of the IM-22 compound, 1.426 (Figure 12). Considering possible errors into account, the difference between the two values is negligible. Therefore, the Hamaker constant *A*, which depends on the difference between the refractive index of the particles and the medium, approaches zero, and the attractive force between the bilayers vanishes. As a result, the repulsive pressure, P_A, drives the bilayers to swell, which leads to an increase of the interlayer spacing, *d*. Similar results were observed by Alexandridis et al.[31] who reported that the lattice parameter of Pluronics in the presence of glycerol can swell up to about 20% from that in the absence of glycerol, while preserving the same microstructure. Much more glycerol will deform or break the lattice structure.

The swelling of the L_α-phase by the increased repulsion with glycerol takes place not only in the L_α-phases, but also in the vesicle phases. The increasing size of vesicles observed in 5% IM-22 system with increasing glycerol concentration can be taken as an evidence for the decreasing attraction of the vesicle membranes. Below 40% glycerol, the remaining repulsion is insufficient to disrupt the membrane structures, so that the system still contains mainly vesicles. From 50 to 60% glycerol content, some vesicles break-up because of increased repulsion exceeding the attractive force that stabilizes the aggregates, and large membrane (bilayer) fragments form. These large vesicles and bilayer fragments align along shear forces, so that we observe shear thinning and flow birefringence in the 5% IM-22 in 60% glycerol system. One can imagine that at even higher glycerol content, almost all the vesicles are broken to bilayer fragments. Then the density difference between the bilayer fragments and the solvent is large enough to induce phase separation, as we observed in the 5% IM-22, 70% glycerol system. In this picture, the upper phase consists of mostly of the bilayer fragments that form the L_α-phase, while the lower phase consists mainly of solvent. However, at even higher glycerol content, the fragments are further disintegrated due to the dehydration of the IM-22 molecules. This is a result of the competition of the glycerol molecules with water to form hydrogen bonds.

It should be pointed out that the observed behavior of Siloxane blockcopolymer system in water/glycerol mixture is of general validity. Other two phase L_1/L_α systems behave in the same way when the refractive index of the bilayers in the L_α-phase is matched by the refractive index of the cosolvent/water mixtures. This will be demonstrated in a forth coming paper in which the L_α-phase is formed by a mixture of normal nonionic surfactant and co-surfactants and the matching of the refractive index is achieved by glycerol and other cosolvents.

Conclusions

The swelling of the L_α-phase of the block copolymer $(EO)_{15}-(PDMS)_{15}-(EO)_{15}$ was investigated in water/glycerol mixtures. Over a large concentration range of 0−60% the compound forms turbid solutions and the mixed solvents. On standing for days and weeks the solutions separate macroscopically into two phases: an isotropic lower aqueous phase and an upper birefringent phase. The turbid solutions contain small unilamellar (SUV) and large multilamellar vesicles (MLV). The bilayers have a thickness of 3.4 nm. For concentrations in the two phase region, the L_α-phase swells with glycerol content until a single phase L_α-region is reached.

The two-phase region shows that in addition to the repulsive forces that are due to undulations of the bilayers, attractive forces exist between the bilayers that balance the repulsive forces at a well defined interlayer spacing. With increasing glycerol concentration the turbid solutions become clear and stable.

This behavior is explained by the reduction of the attractive forces between the vesicles by the increasing glycerol content. The refractive index contrast between the bilayers and the solvent is completely lost at 60% glycerol, and the phases become stable.

Acknowledgment. We greatly acknowledge the Wacker Company for providing the compound IM-22. The direct-

imaging cryo-TEM work was performed in the Hannah and George Krumholz Laboratory for Advanced Microscopy, part of the Technion Project on Complex Fluids, Microstructure and Macromolecules. We also thank Dr. Aihua Zou for providing Figures 1, 2, 7, and 9. Y.T. thanks the von Humboldt Foundation for the Meitner-Von Humboldt Prize.

Note Added after ASAP Publication. This article was released ASAP on May 10, 2007. Equations 3, 4, 5, and surrounding text have been revised. References 38 and 40 have been added. The corrected version was posted on May 25, 2007.

References and Notes

(1) Schmidt, G. *Tenside, Surfactants, Deterg.* **1990**, *27*, 324.
(2) Klein, K.-D.; Schaefer, D.; Lersch, P. *Tenside, Surfactants, Deterg.* **1994**, *31*, 115.
(3) Oertel, G., Ed. In *Polyurethane Handbook*; Carl Hanser: Munich, 1985.
(4) Fink, H. F. *Tenside, Surfactants, Deterg.* **1991**, *28*, 306.
(5) Kobayashi, R.; Yabe, S.; Nomura, T. *Polym. Adv. Technol.* **1997**, *8*, 351.
(6) Bonner, M. P.; Wilson, J. I. B.; Burnside, B. M.; Reuben, R. L.; Gengenbach, T. R.; Crisser, H. J.; Beamson, G. *J. Mater. Sci.* **1998**, *33*, 4843.
(7) Krupers, M. J.; Bartelink, C. F.; Gruenhauer, H. J. M.; Moeller, M. *Polymer* **1998**, *39*, 2049.
(8) Hill, R. M., Ed. In *Siloxane Surfactants*; Surfactant Science Series; Marcel Dekker, Inc.: New York, 1999; Vol. 86.
(9) Svitova, T. H.; Hill, R. M. *Langmuir* **1996**, *12*, 1712.
(10) Li, X.; Washenberger, R. M.; Scriven, L. E.; Davis, H. T.; Hill, R. M. *Langmuir* **1999**, *15*, 2267.
(11) Stuermer, A.; Thunig, C.; Hoffmann, H.; Gruening, B. *Tenside, Surfactants, Deterg.* **1994**, *31*, 90.
(12) Gradzielski, M.; Hoffmann, H.; Robisch, P.; Ulbricht, W.; Gruening, B. *Tenside, Surfactants, Deterg.* **1990**, *27*, 366.
(13) Lin, Z.; Hill, R. M.; Davis, H. T.; Scriven, L. E.; Talmon, Y. *Langmuir* **1994**, *10*, 1008.
(14) Kunieda, H. K.; Uddin, M. H.; Horii, M.; Furukawa, H.; Harashima, A. *J. Phys. Chem. B* **2001**, *105*, 5419.
(15) Lin, Y.; Alexandridis, P. *Langmuir* **2002**, *18*, 4220.
(16) Yan, Y.; Hoffmann, H.; Drechsler, M.; Talmon, Y.; Makarsky, E. *J. Phys. Chem. B* **2006**, *110*, 5621.
(17) Martin, M.; Swaebrick, J., Ananthapadamanabhan, K. P., Eds. In *Physical Pharmacy*; Lea & Febiger Press: Philadelphia, PA, 1983.
(18) Sjöberg, M.; Warnheim, T. *Surfactant Sci. Ser.* **1997**, *67*, 179.
(19) Corrin, M. L.; Hrakins, W. D., *J. Chem. Phys.* **1946**, *14*, 640.
(20) Paola, G. Di; Belleau, B. *Can. J. Chem.* **1975**, *53*, 3452.
(21) Aramaki, K.; Olsson, U.; Yamaguchi, Y.; Kunieda, H. *Langmuir* **1999**, *15*, 6226.
(22) Martino, A.; Kaler, E. W. *Colloids Surf. A* **1995**, *99*, 91.
(23) Lin, Y.; Alexandridis, P. *J. Phys. Chem. B* **2002**, *106*, 12124.
(24) Takisawa, N.; Thomason, M.; Bloor, D. M.; Wyn-Jones, E. *J. Colloid Interface Sci.* **1993**, *157*, 77.
(25) Palepu, R.; Gharibi, H.; Bloor, D. M.; Wyn-Jones E. *Langmuir* **1993**, *9*, 110.
(26) Bakshi M. S. *J. Chem. Soc. Faraday Trans.* **1993**, *89*, 4323.
(27) Cantú, L.; Corti, M.; Degiorgio, V.; Hoffmann, H.; Ulbricht, W. *J. Colloid Interface Sci.* **1987**, *116*, 384.
(28) Ionescu, L. G.; Trindade, V. L.; de Douza, E. F. *Langmuir* **2000**, *16*, 988.
(29) D'Erricl, G.; Ciccarelli, D.; Ortona, O. *J. Colloid Interface Sci.* **2005**, *286*, 747.
(30) Iwanaga, T.; Suzuki, M.; Kunieda, H. *Langmuir* **1998**, *14*, 5775.
(31) Alexandridis, P.; Ivanova, R.; Lindman, B. *Langmuir* **2000**, *16*, 3676.
(32) Borst, J. W.; Hink, M. A.; van Hoek, A.; Visser, A. J. W. G. *J. Fluoresc.* **2005**, *15*, 153.
(33) Vezenov, D. V.; Mayers, B. T.; Wolfe, D. B.; Whitesides, G. M. *Appl. Phys. Lett.* **2005**, *86*, 041104.
(34) http://www.texloc.com/closet/cl_refractiveindex.html.
(35) Talmon, Y. In *Modern Characterization Methods of Surfactant Systems*; Binks, B. P., Ed.; Marcel Dekker: New York, 1999; p 147.
(36) Zhang, Y.; Schmidt, J.; Talmon, Y.; Zakin, J. *J. Colloid Interface Sci.* **2005**, *286*, 696.
(37) Mortensen, K.; Talmon, Y. *Macromolecules* **1995**, *28*, 8829.
(38) Parsegian, V. A. In *Van der Waals Forces*; Cambridge University Press: Cambridge, UK, 2005.
(39) Hiemenz, P. C. In *Principles of Colloid and Surface Chemistry*, 2nd revised ed. ; Marcel Dekker Ltd.: New York, 1985.
(40) Helfrich, W. *Z. Naturforsch.* **1978**, *A33*, 305−315.